Electronic Supplementary Information

Temperature- and excitation wavelength-dependent emission in a manganese(II) complex

Alexei S. Berezin,[a] Katerina A. Vinogradova,*[a,b] Vladimir A. Nadolinny,[a] Taisiya S. Sukhikh,[a,b] Viktor P. Krivopalov,[c] Elena B. Nikolaenkova[c] and Mark B. Bushuev**[a,b]

[a] Nikolaev Institute of Inorganic Chemistry, Siberian Branch of Russian Academy of Sciences, 3, Acad. Lavrentiev Ave., Novosibirsk, 630090, Russia, E-mail addresses: kiossarin@mail.ru (K. A. Vinogradova), bushuev@niic.nsc.ru, mark.bushuev@gmail.com (M. B. Bushuev); Fax: +7 383 330 94 89; Tel: +7 383 316 51 43.

[b] Novosibirsk State University, 2, Pirogova str., Novosibirsk, 630090, Russia.

[c] N. N. Vorozhtsov Novosibirsk Institute of Organic Chemistry, Siberian Branch of Russian Academy of Sciences, 9, Acad. Lavrentiev Ave., Novosibirsk, 630090, Russia.

Table of contents

Table S1. Crystallographic data for **1b** and **1c**.

Compound	**[**MnL_2Cl_2]·H_2O·EtOH (**1b**)	[MnL_2Cl_2]·Me_2CO (**1c**)
Empirical formula	$C_{50}H_{54}Cl_2MnN_{10}O_2$	$C_{51}H_{52}Cl_2MnN_{10}O$
Formula weight	951.8	946.9
Temperature, K	150(2)	298 (RT)
Crystal system	Monoclinic	Monoclinic
Space group	$P2_1/n$	$C2/c$
Unit cell dimensions *a*, [Å]	11.6451(3)	19.279(4)
b, [Å]	17.7149(5)	13.195(4)
c, [Å]	23.7054(7)	20.968(7)
α, [°]	90	90
β, [°]	101.5090(10)	115.383(17)
γ, [°]	90	90
Volume [Å^3]	4791.9(2)	4819(3)
Z	4	4
Density (calcd.) [g cm^{-3}]	1.317	1.305
Abs. coefficient [mm^{-1}]	0.438	0.434
F(000)	1984	1980
Crystal size [mm^3]	0.20×0.20×0.05	0.28×0.13×0.13
$2\theta_{max}$ [°]	51.38	51.48
Index range	–14≤*h*≤14, –21≤*k*≤21, –28≤*l*≤28	–23≤*h*≤17, –15≤*k*≤16, –25≤*l*≤25
Reflections collected	59487	14805
Independent reflections	9107 [R(int) = 0.0831]	4523 [R(int) = 0.0587]
Reflections, I ≥ 2σ(I)	5862	3391
Completness to θ [%]	99.9	98.0
Parameters	582	314
Final R indices [I > 2σ(I)]	R_1 = 0.0582, wR_2 = 0.1331	R_1 = 0.0446, wR_2 = 0.1181
R indices (all data)	R_1 = 0.1062, wR_2 = 0.1563	R_1 = 0.0654, wR_2 = 0.1296
GoF	1.024	1.016
Residual electron density (min / max, e/Å^3)	-0.508 / 0.798	-0.335 / 0.340

Table S2. Selected bond lengths (Å) and angles (°) for **1b** and **1c.**

1b		**1c**	
Mn1–Cl1	2.4356(9)	Mn1–Cl1	2.4631(11)
		Mn1–Cl2	2.4524(10)
Mn1–N11	2.500(2)	Mn1–N11	2.508(3)
		Mn1–N21	2.415(3)
Mn1–N13	2.2179(18)	Mn1–N13	2.188(3)
		Mn1–N23	2.189(3)
Cl1–Mn1–Cl1	102.44(5)	Cl1–Mn1–Cl2	98.85(4)
N11–Mn1–Cl1	159.08(5)	N11–Mn1–Cl1	89.44(7)
		N21–Mn1–Cl1	158.77(7)
N11'–Mn1–Cl1	93.11(5)	N11–Mn1–Cl2	164.10(7)
		N21–Mn1–Cl2	95.36(7)
N11–Mn1–N11'	75.81(9)	N11–Mn1–N21	80.80(9)
N13–Mn1–Cl1	99.50(6)	N13–Mn1–Cl1	99.36(9)
		N23–Mn1–Cl1	92.90(8)
N13–Mn1–Cl1'	95.34(5)	N13–Mn1–Cl2	96.05(9)
		N23–Mn1–Cl2	98.26(8)
N13–Mn1–N11	92.81(7)	N13–Mn1–N11	69.08(10)
		N13–Mn1–N21	94.72(11)
N13–Mn1–N11'	68.04(6)	N23–Mn1–N11	94.83(10)
		N23–Mn1–N21	69.40(9)
N13–Mn1–N13'	156.23(10)	N13–Mn1–N23	159.48(11)
N11–N12–C14–N13	16.7(3)	N11–N12–C14–N13	28.3(4)
		N21–N22–C24–N23	20.0(4)

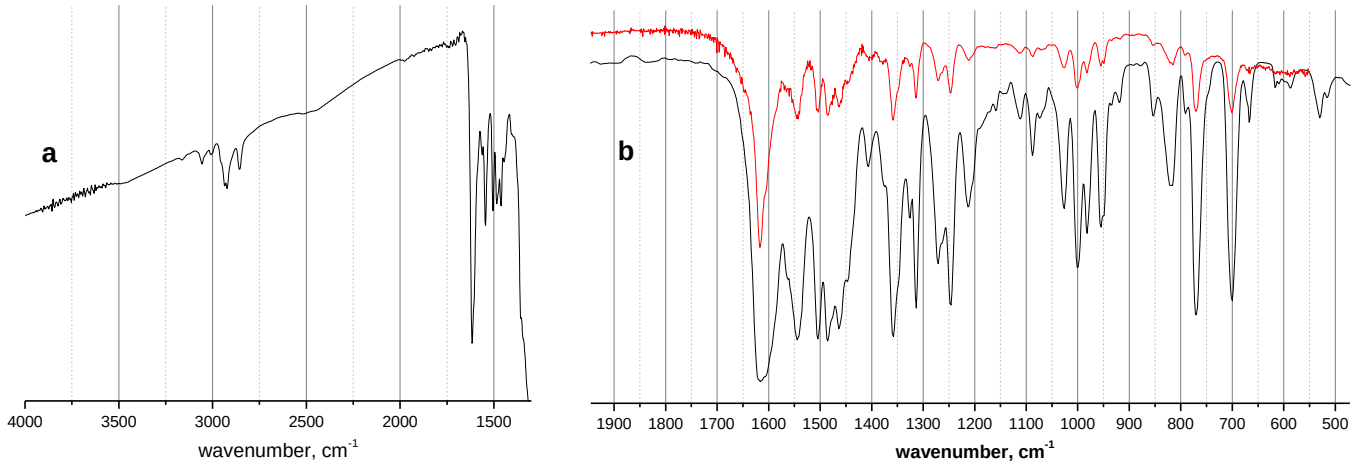

Fig. S1. IR spectrum of $[MnL_2Cl_2]\cdot H_2O$ recorded in fluorinated oil (a). IR spectra of two different simples of the complex $[MnL_2Cl_2]\cdot H_2O$ recorded in KBr matrix (b).

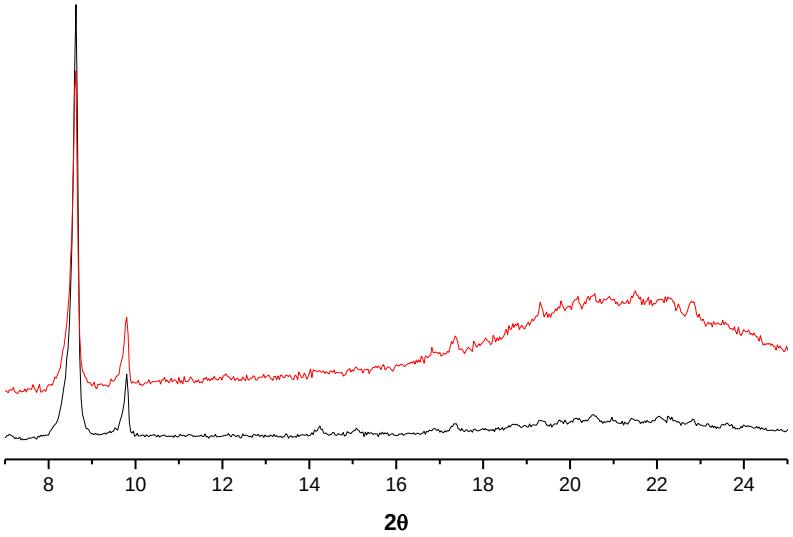

Fig. S2. X-ray powder diffraction patterns of two different simples of the complex $[MnL_2Cl_2]\cdot H_2O$. Black line is the aged sample, red line is the freshly prepared sample.

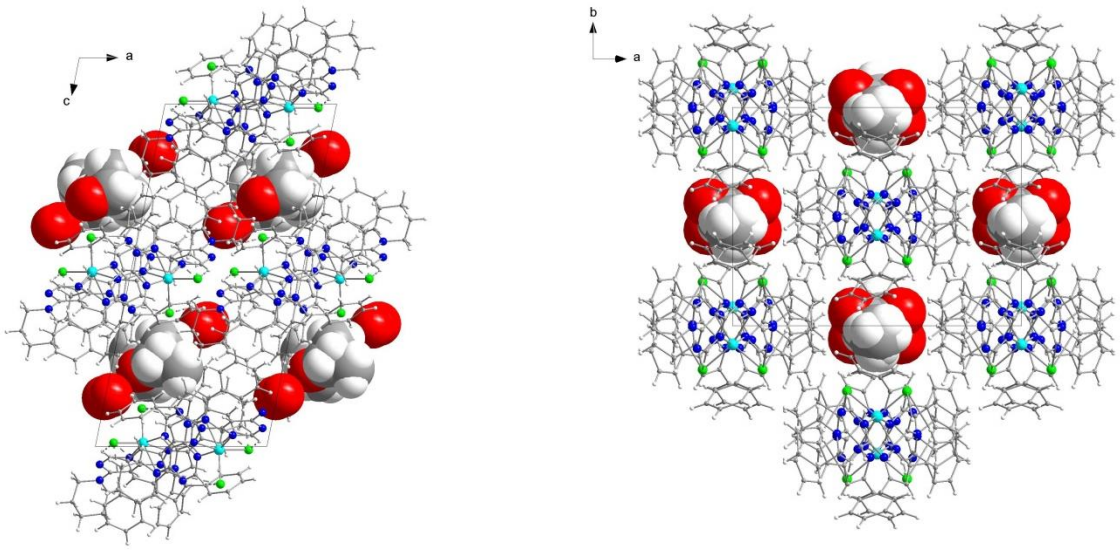

Fig. S3. Crystal packing of **1b** (left) and **1c** (right) showing relative arrangement of disordered acetone, water and ethanol molecules in space-filling model.

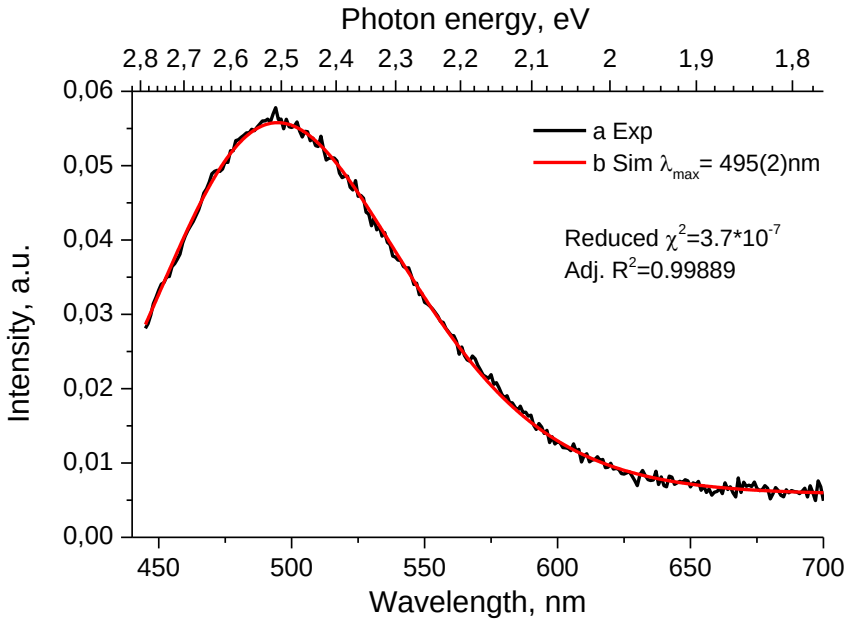

Fig. S4. Emission spectrum of polycrystalline $[MnL_2Cl_2]\cdot H_2O$ at 300 K, λ_{Ex} = 410 nm. This spectrum (λ_{Ex} = 410 nm) is described by a single Gauss function with the maximum at 495(2) nm (red line).

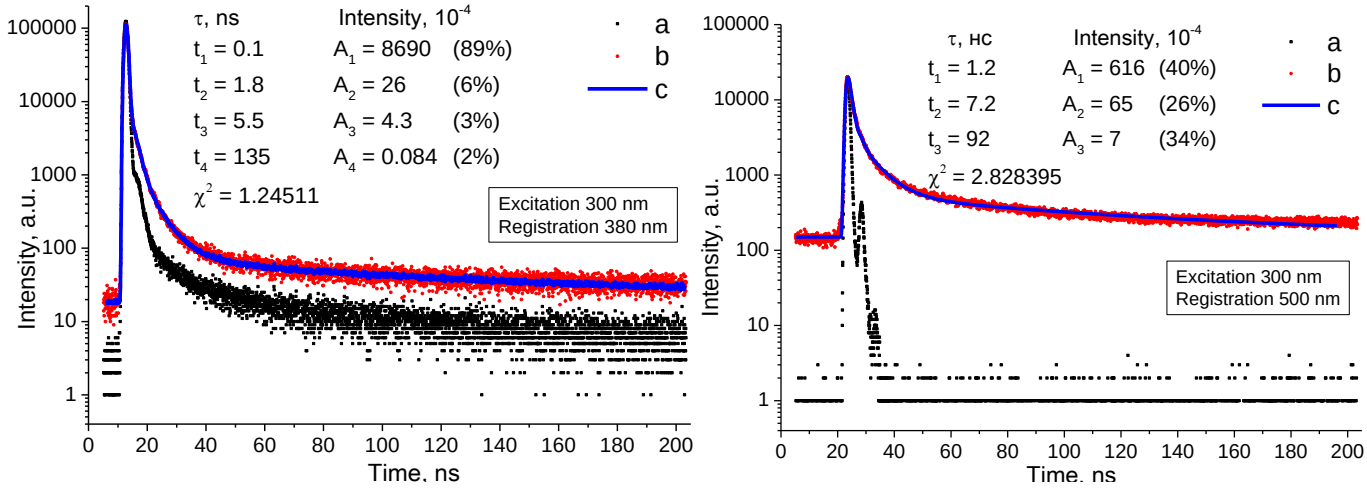

Fig. S5. Kinetic curves of the photoluminescence for $[MnL_2Cl_2]\cdot H_2O$ in the solid state at 295 K: excitation at 300 nm and registration at 380 nm (left), excitation at 300 nm and registration at 500 nm for the 495 nm band (right); a) instrument response function, b) experimental points and c) approximation.

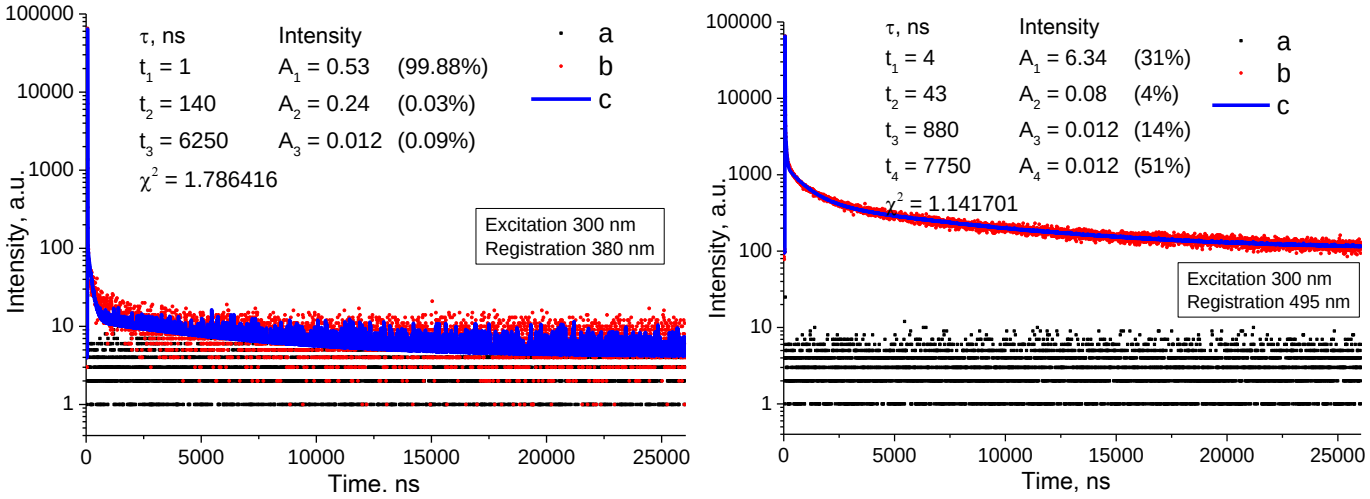

Fig. S6. Kinetic curves of the photoluminescence for $[MnL_2Cl_2]\cdot H_2O$ in the solid state at 295 K: excitation at 300 nm and registration at 380 nm (left), excitation at 300 nm and registration at 500 nm for the 495 nm band (right); a) instrument response function, b) experimental points and c) approximation.

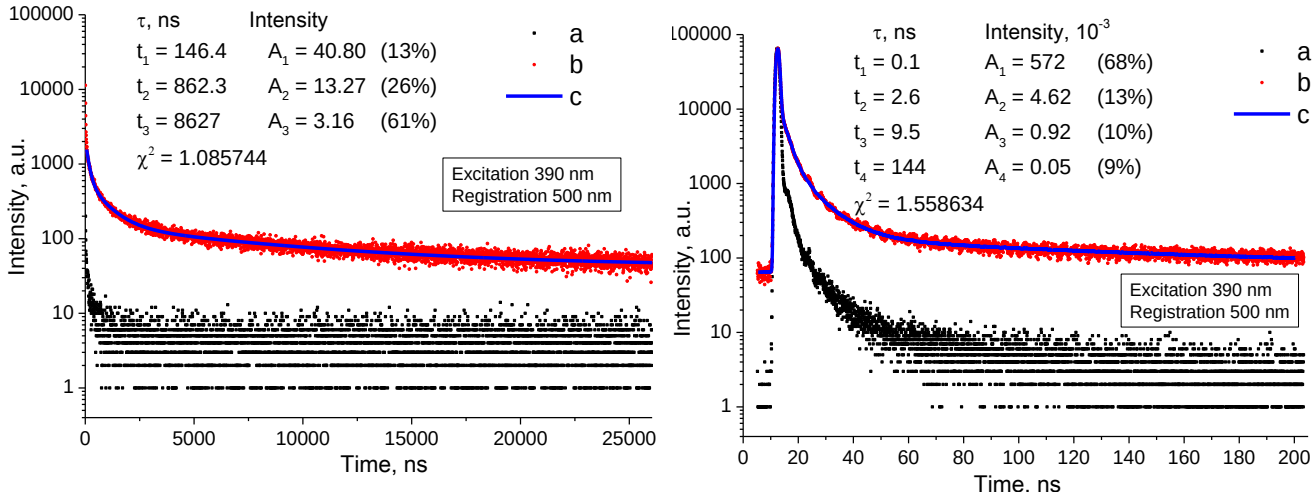

Fig. S7. Kinetic curves of the photoluminescence for $[MnL_2Cl_2]\cdot H_2O$ in the solid state at 295 K: excitation at 390 nm and registration at 500 nm for the 495 nm band; a) instrument response function, b) experimental points and c) approximation.

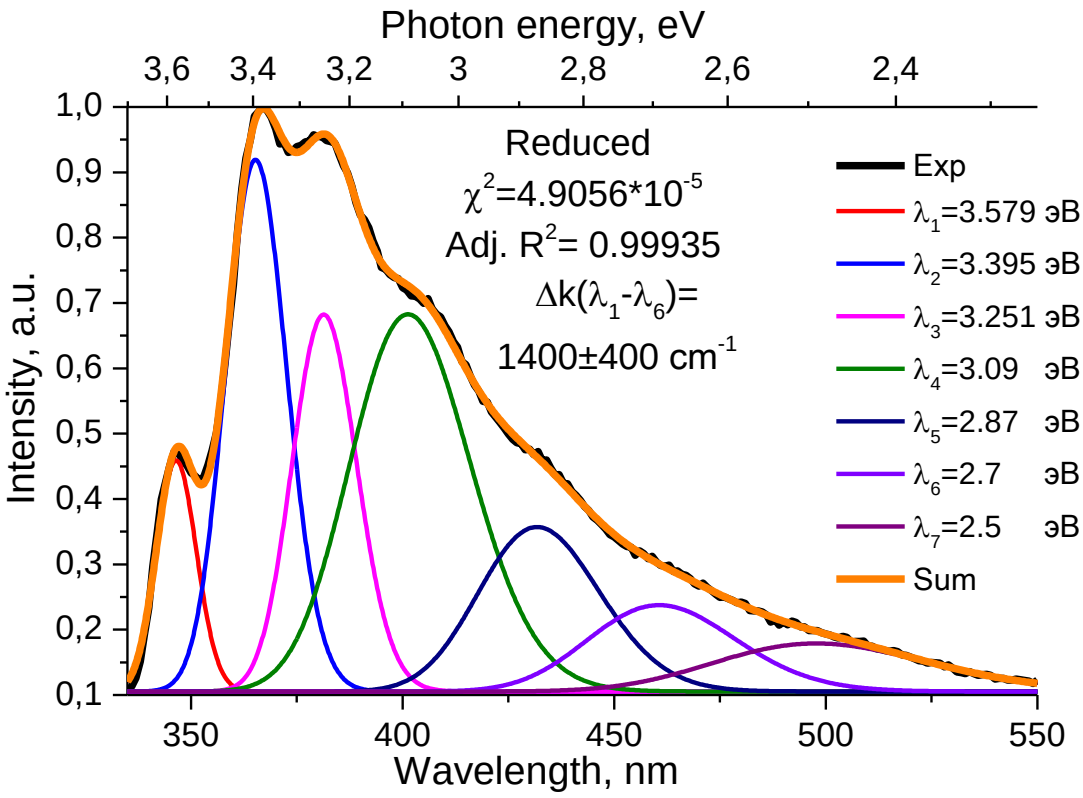

Fig. S8. The emission spectrum of polycrystalline $[MnL_2Cl_2]\cdot H_2O$ (λ_{Ex} = 300 nm) recorded at 77 K. The emission spectrum is resolved into seven Gauss functions.

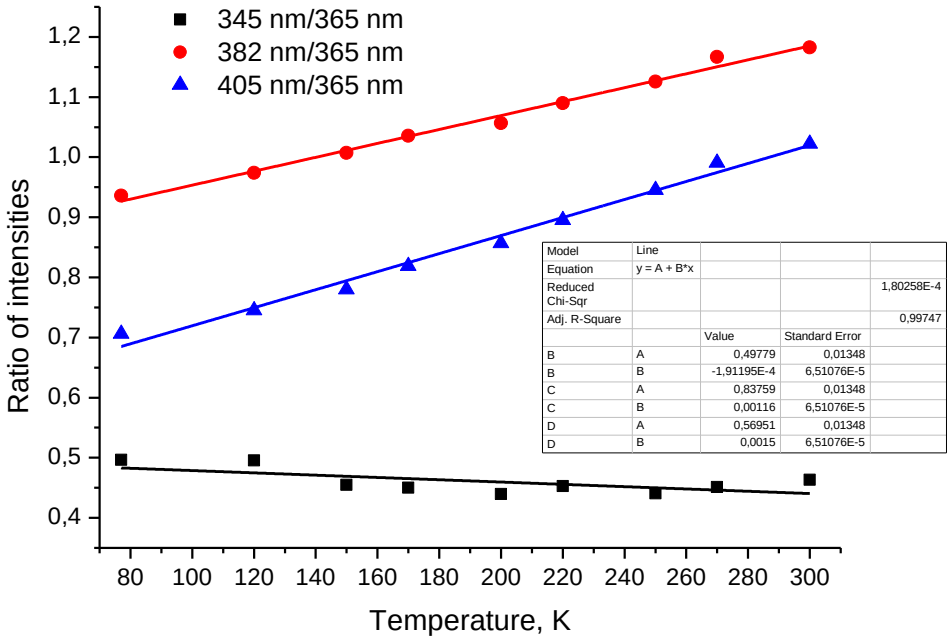

Fig. S9. Temperature dependence of the intensities ratio of the 345 nm and 365 nm lines (black); 382 nm and 365 nm lines (red); 405 nm and 365 nm lines (red) for $[MnL_2Cl_2]\cdot H_2O$.

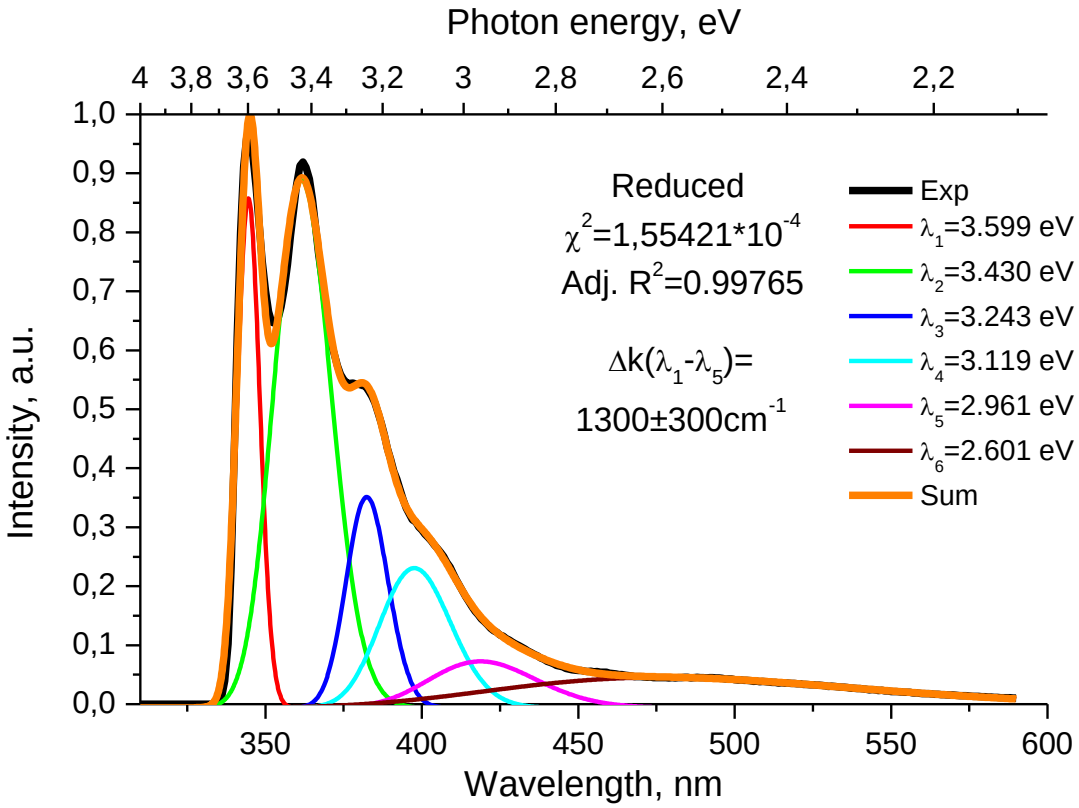

Fig. S10. The emission spectrum of polycrystalline L (λ_{Ex} = 300 nm) recorded at 77 K. The emission spectrum is resolved into six Gauss functions.

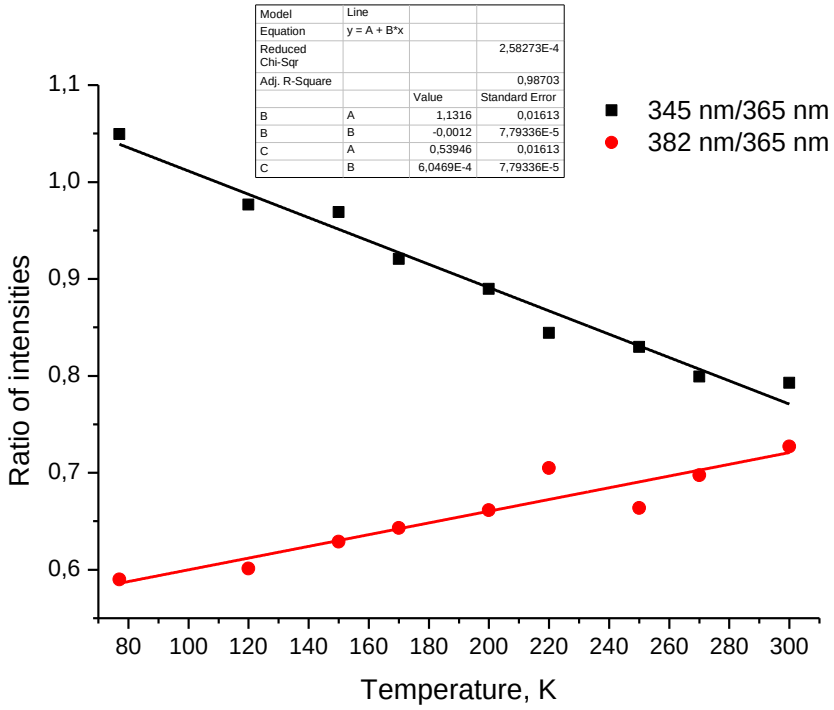

Fig. S11. Temperature dependence of the intensities ratio of the 345 nm and 365 nm lines (black); 382 nm and 365 nm lines (red) for L.

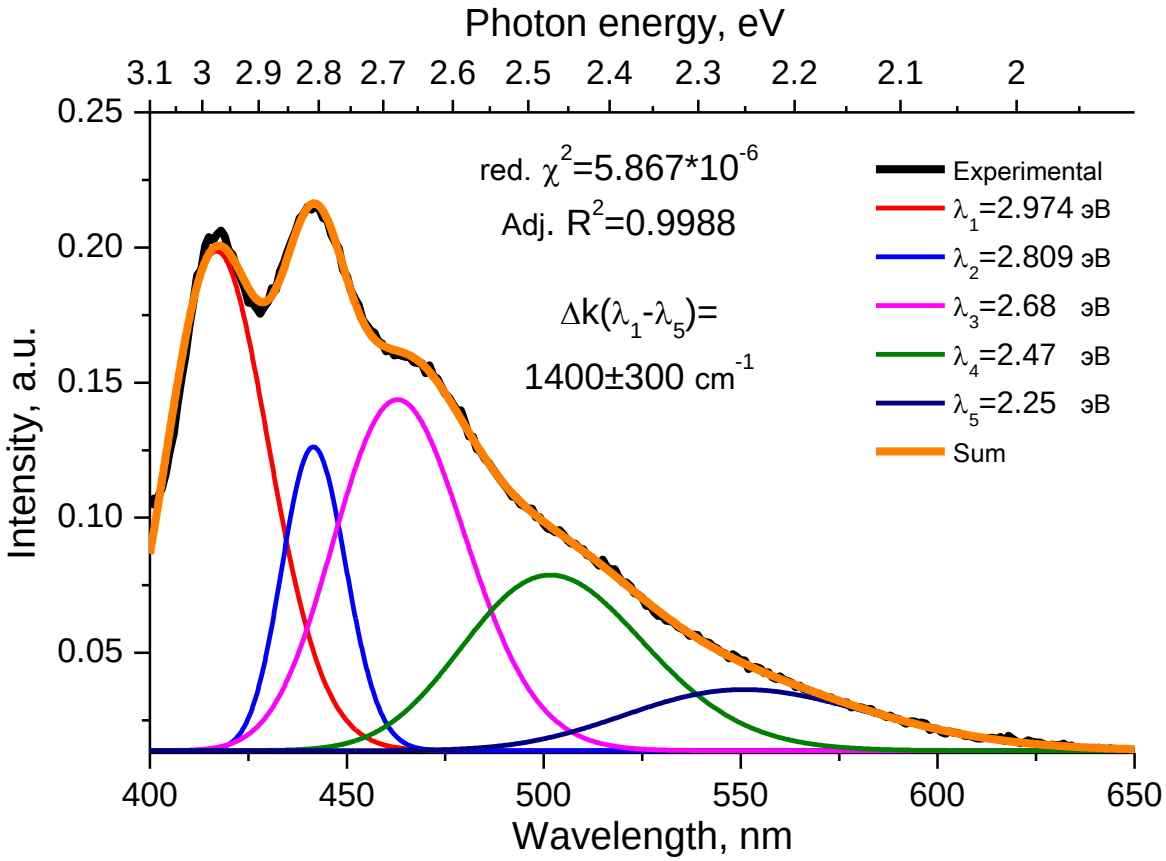

Fig. S12. The emission spectrum of polycrystalline $[MnL_2Cl_2]\cdot H_2O$ (λ_{Ex} = 380 nm) recorded at 77 K. The emission spectrum is resolved into five Gauss functions, the 495(2) nm band is absent. The quintet corresponds to the vibrational structure with $\Delta k = 1400 \pm 300\ cm^{-1}$ (0-1 is the main transition). However, the positions of the components of the quintet differ from the positions of the sextet observed upon excitation at 300 nm (Fig. S8).

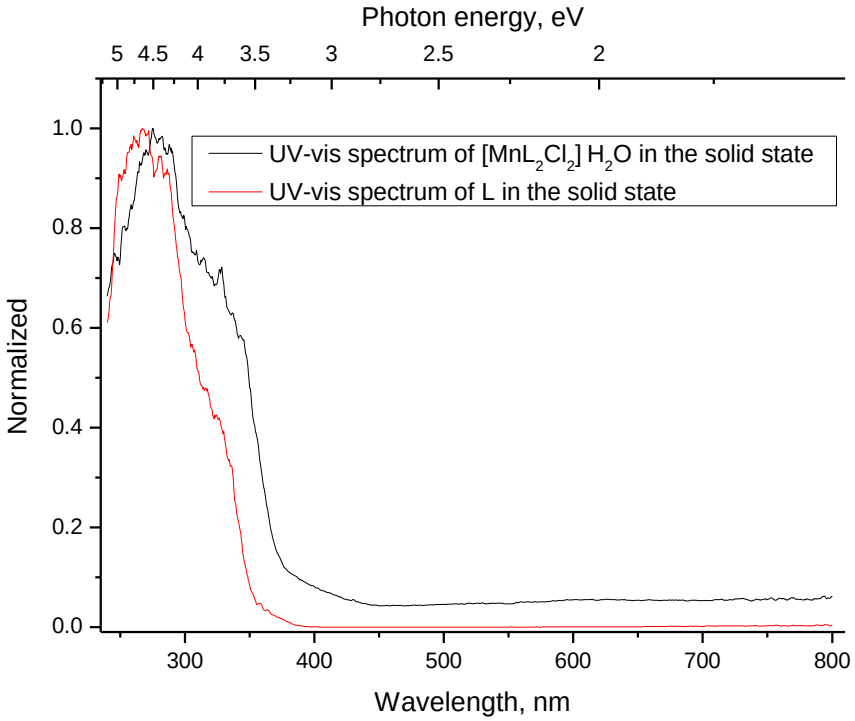

Fig. S13. Normalized UV-vis spectra (the Kubelka-Munk function) of $[MnL_2Cl_2]\cdot H_2O$ and L in the solid state.

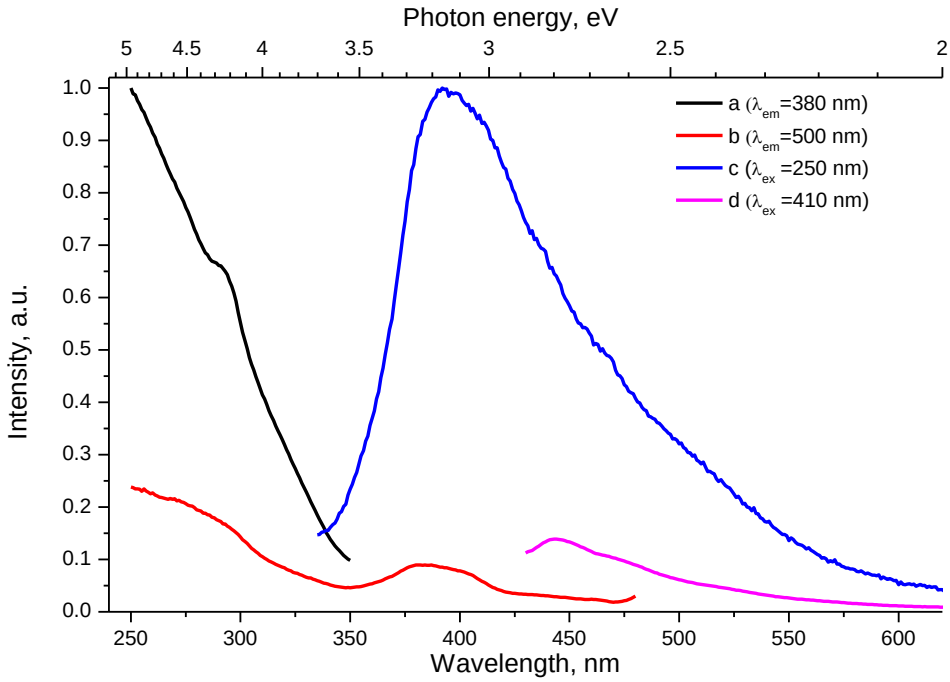

Fig. S14. Excitation and emission spectra of freshly prepared $[MnL_2Cl_2]\cdot Me_2CO$ at 300 K.

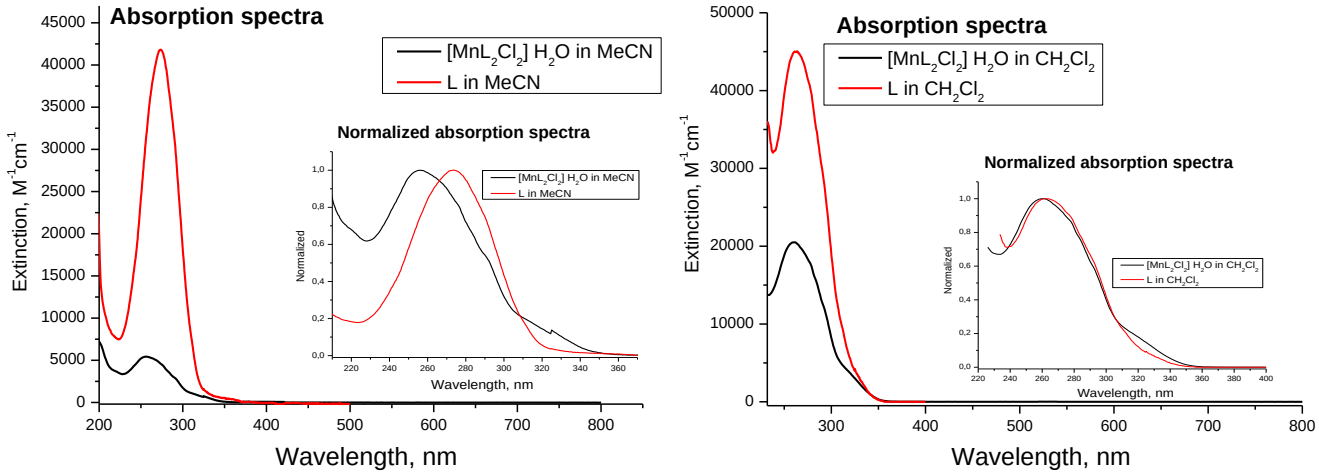

Fig. S15. Absorption spectra of $[MnL_2Cl_2]\cdot H_2O$ and L in acetonitrile and dichloromethane solutions.

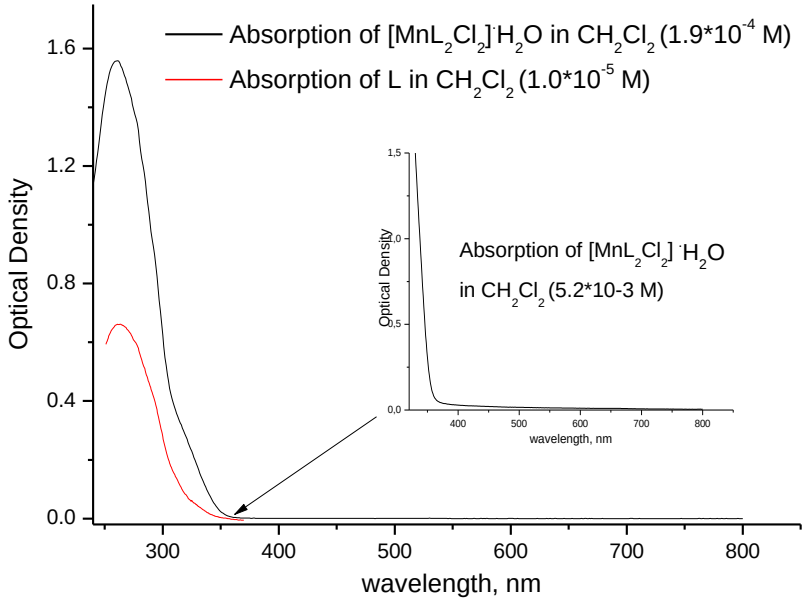

Fig. S16. Absorption spectra of $[MnL_2Cl_2]\cdot H_2O$ and L in dichloromethane solutions.

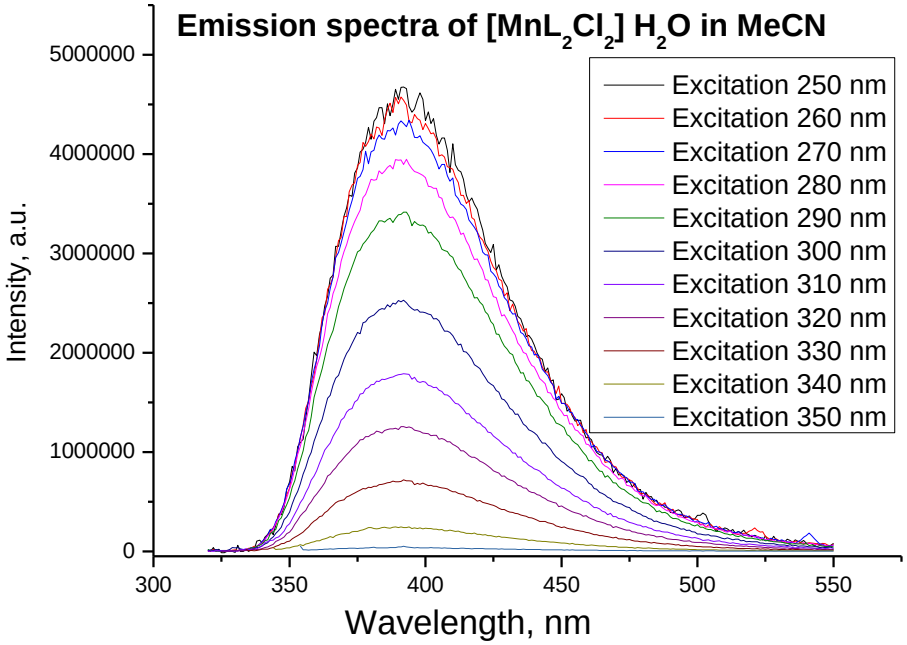

Fig. S17. Emission spectra of $[MnL_2Cl_2]\cdot H_2O$ in acetonitrile solution.

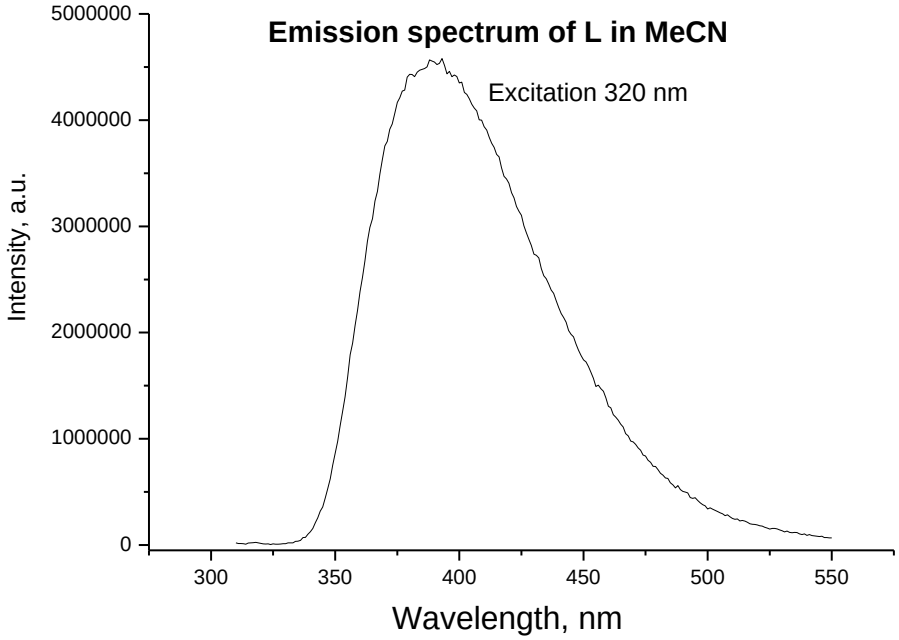

Fig. S18. Emission spectrum of L in acetonitrile solution.

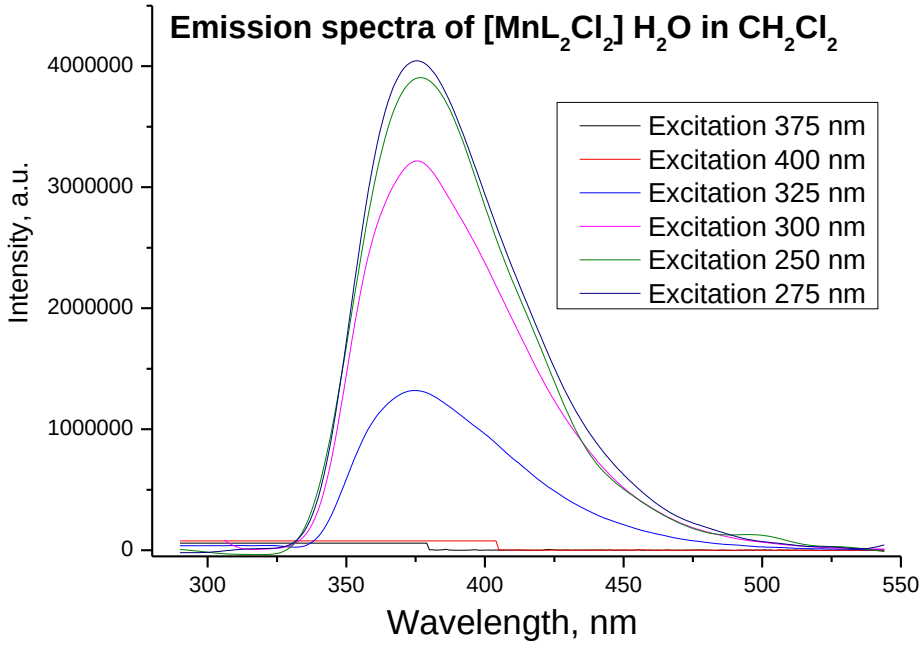

Fig. S19. Emission spectra of $[MnL_2Cl_2]\cdot H_2O$ in dichloromethane solution.

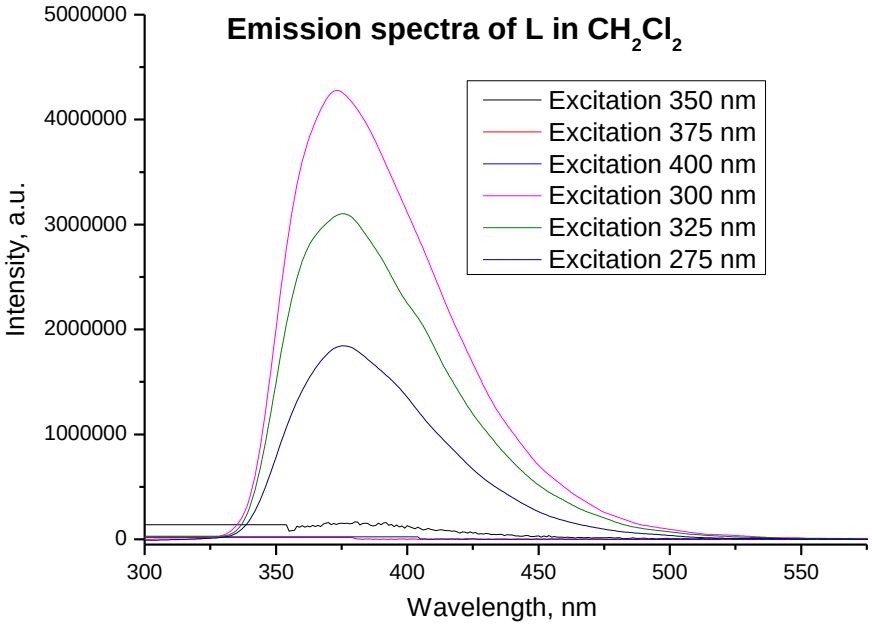

Fig. S20. Emission spectra of L in dichloromethane solution.

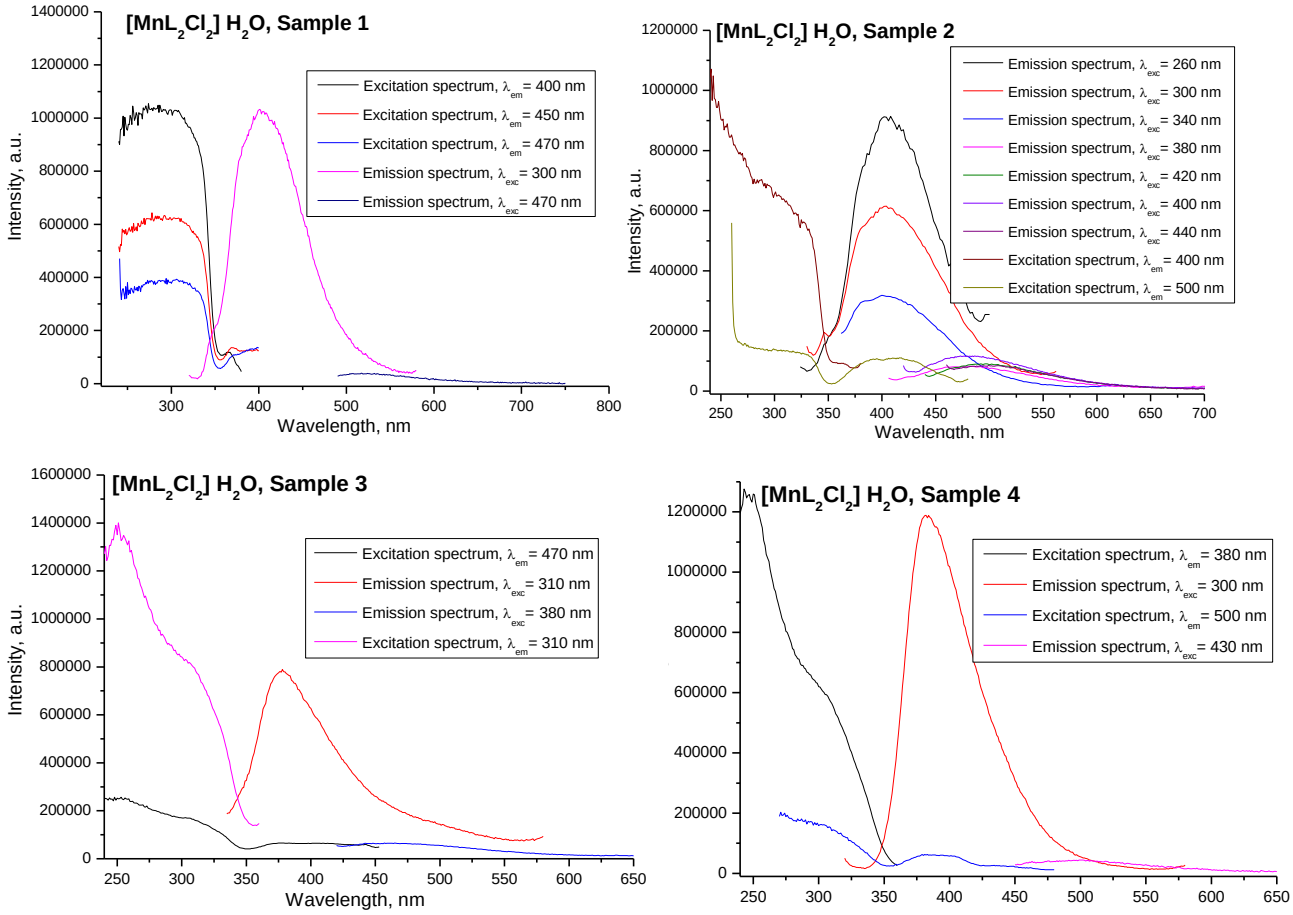

Fig. S21. Emission and excitation spectra of four different samples of $[MnL_2Cl_2]\cdot H_2O$.

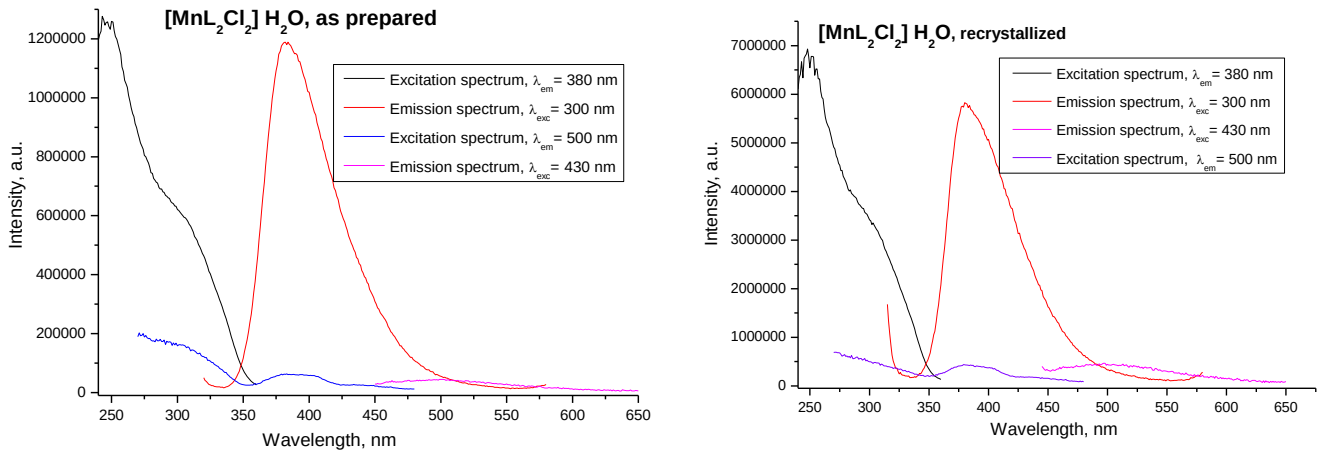

Fig. S22. Emission and excitation spectra of $[MnL_2Cl_2]\cdot H_2O$ of as prepared sample (left) and recrystallized sample (right).

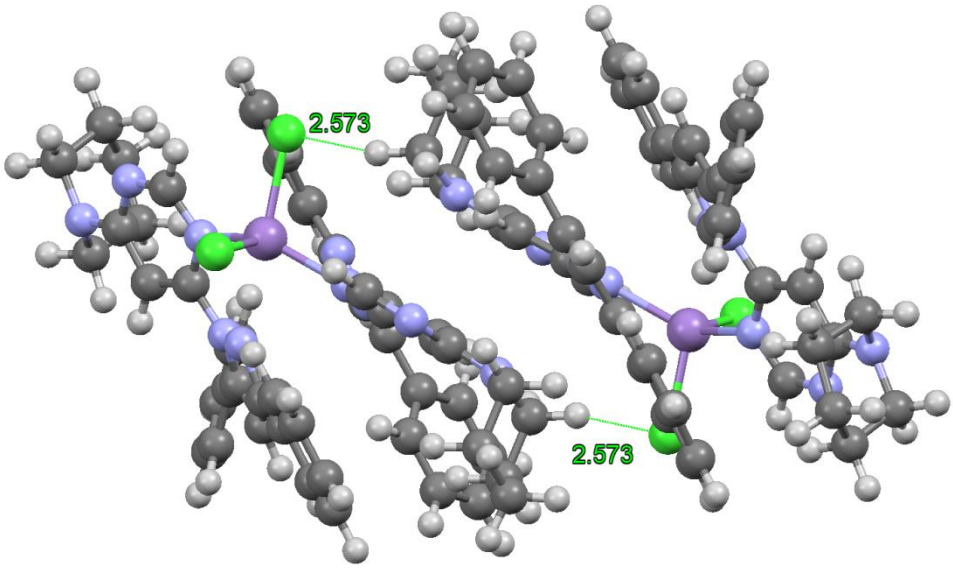

Fig. S23. DFT calculated (BP86/TZP) molecular structure of dimeric unit $[MnL_2Cl_2]_2$.

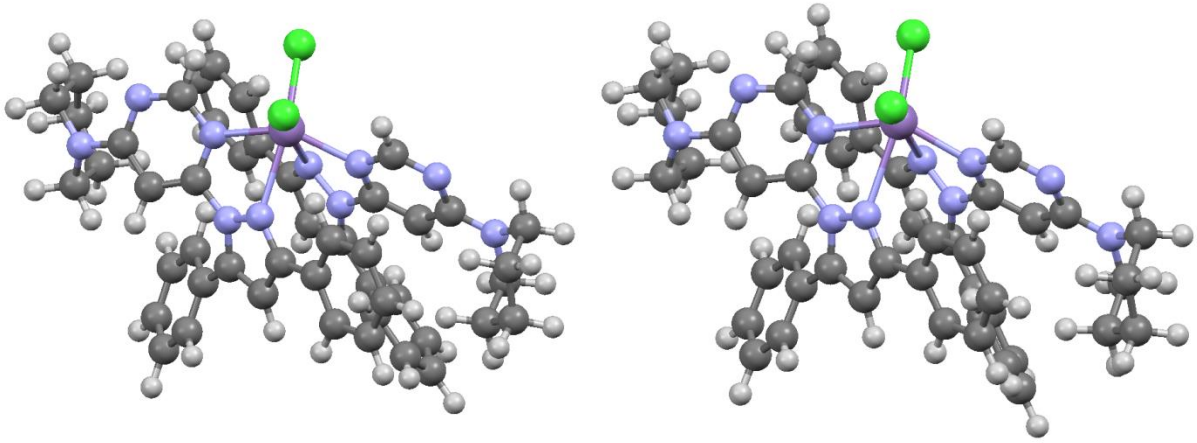

Fig. S24. Experimental (a) and calculated (BP86/TZP) (b) molecular structures.

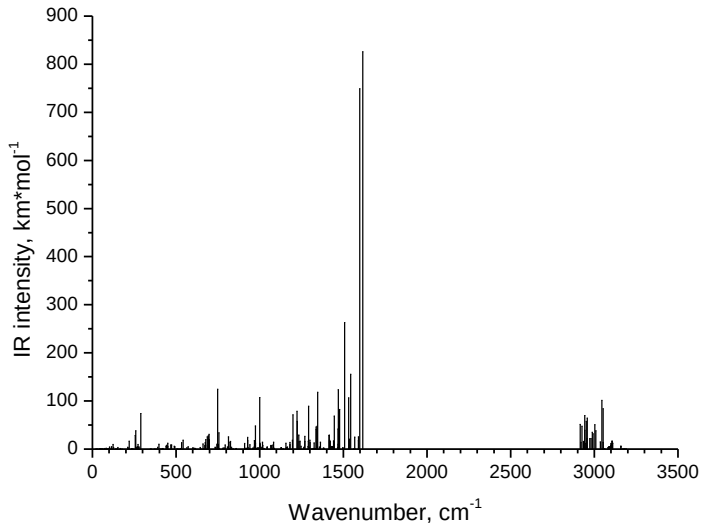

Fig. S25. IR-spectrum obtained by simulation in ADF with BP86 functional after numerical recalculation (1 Debye^2-angstrom^{-2}-amu^{-1} = 42.2561 km*mol^{-1}).

a)

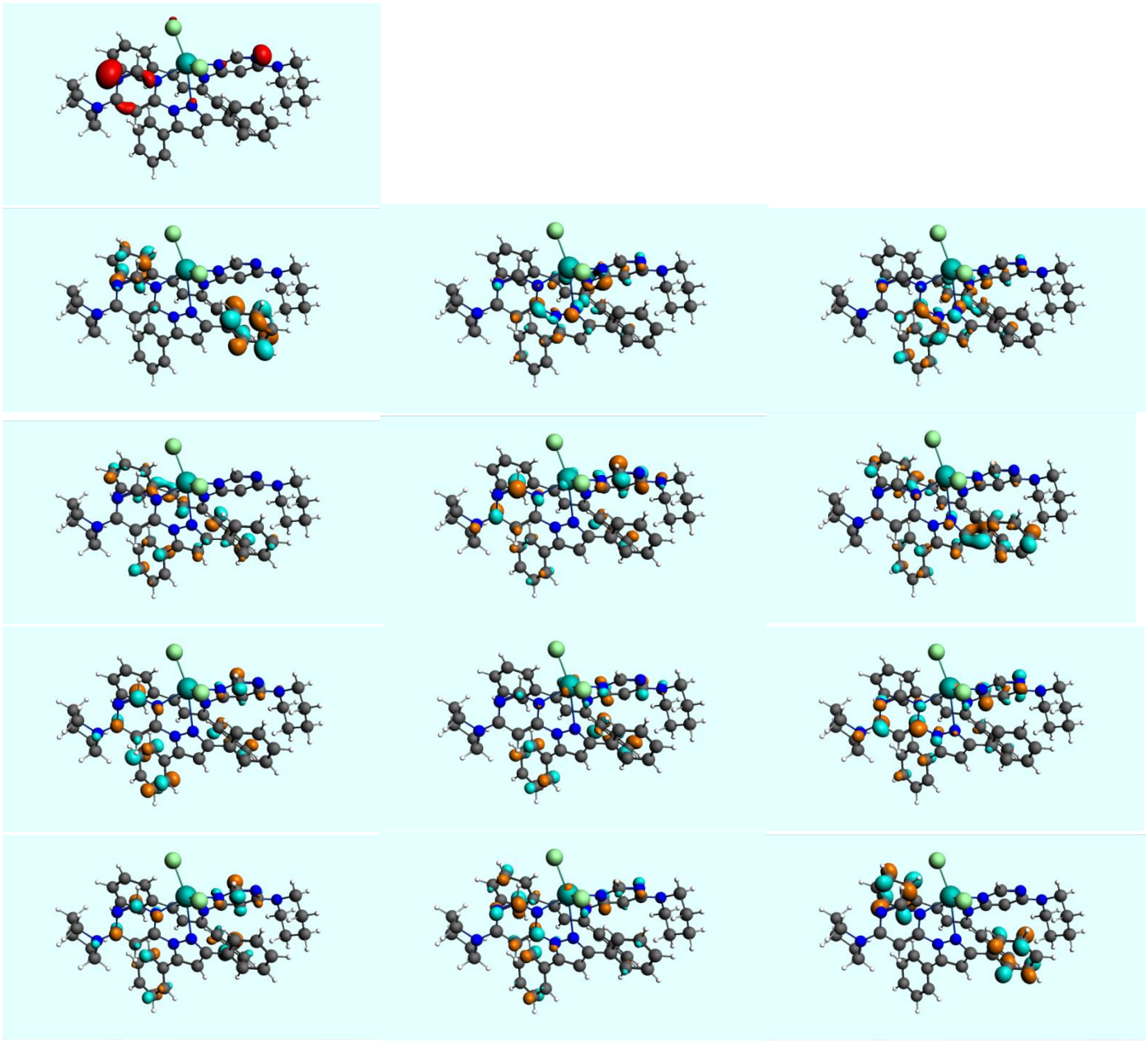

b)

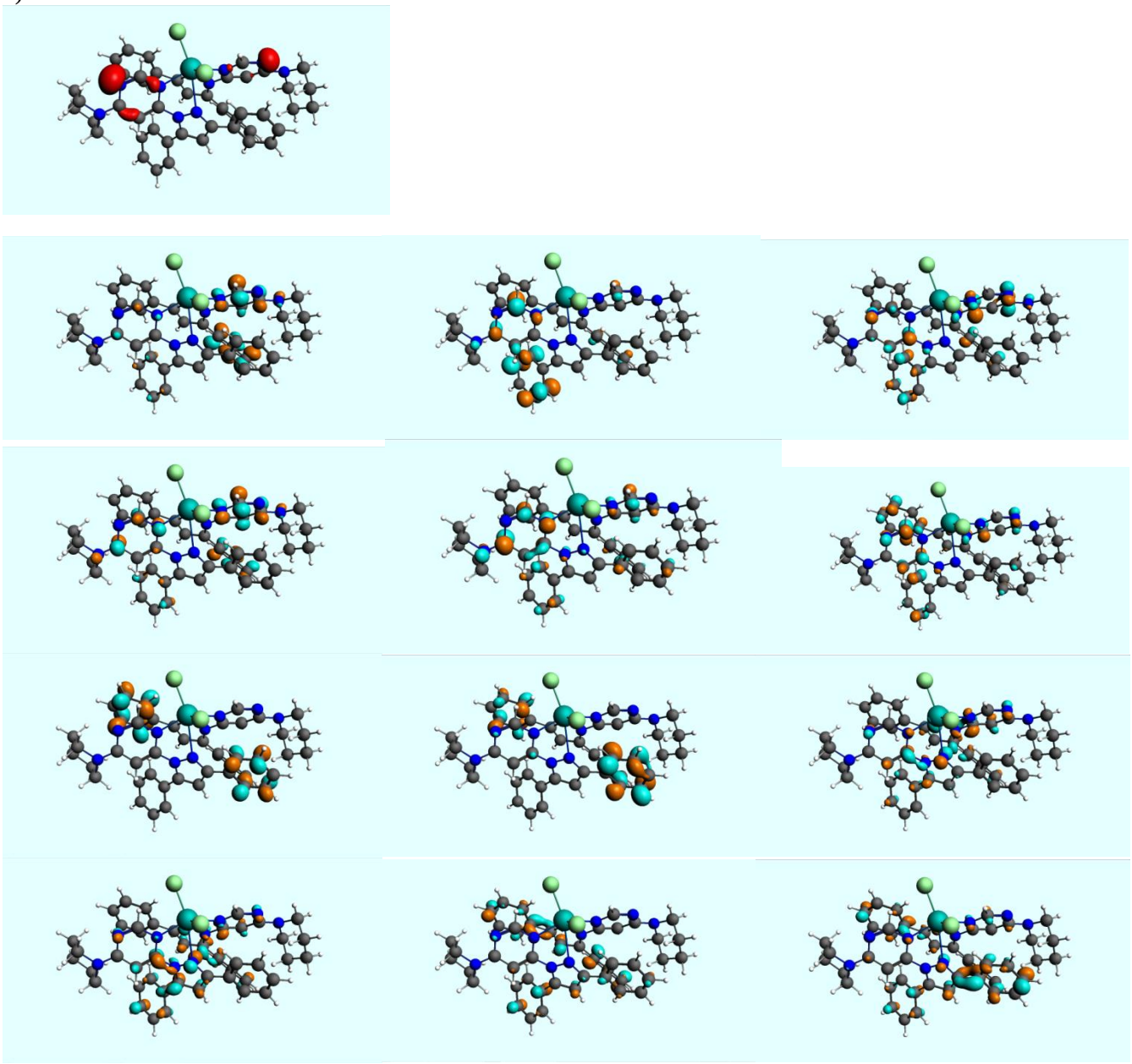

Fig. S26. HOMOs and LUMOs of n to π* transitions.

Each molecular orbital consists of a large number of atomic orbitals. The molecular orbitals participate in excitation. Therefore, a large number of atomic orbitals participate in each transition. Moreover, a large number of unoccupied MOs are involved in each transition. We have shown HOMOs (spin-up (a) and spin-down (b)) which consist of nitrogen lone-electron pair orbitals and lying in the UV-Vis excitation range. Also, we have shown π* LUMOs to which the transitions occur (from the HOMOs).

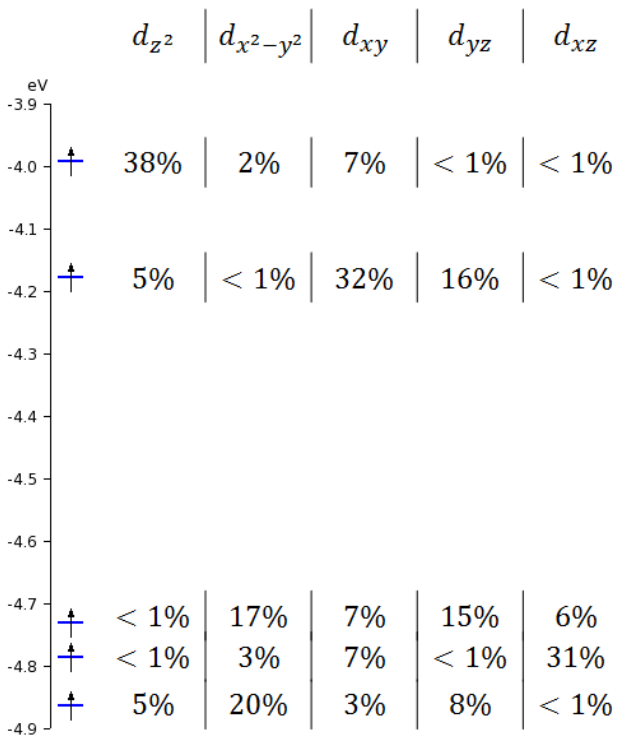

Fig. S27. The contributions of d orbitals to MOs.

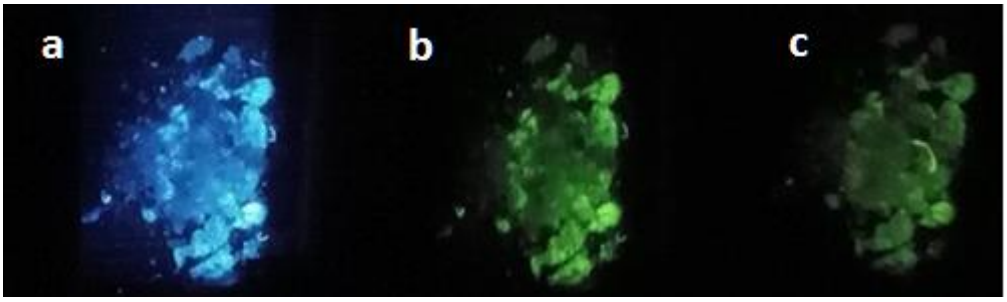

Fig. S28. The photographies of the emission emission of $[MnL_2Cl_2]\cdot H_2O$: a) λ_{ex} = 300 nm, b) λ_{ex} = 300 nm with the light filter 500 nm, c) λ_{ex} = 430 nm with the light filter 500 nm.

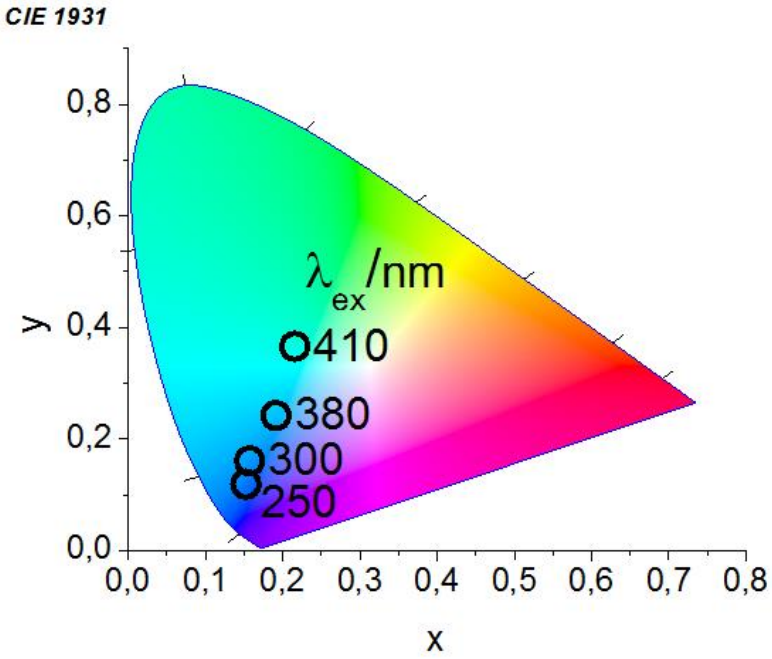

Fig. S29. CIE-1931 chromaticity diagram for polycrystalline $[MnL_2Cl_2]\cdot H_2O$.